

# Kinetic investigation of a controlled drug delivery system based on alginate scaffold with embedded voids

Journal of Applied Biomaterials & Functional Materials  
April-June: 1–8  
© The Author(s) 2019  
Article reuse guidelines:  
sagepub.com/journals-permissions  
DOI: 10.1177/2280800018817462  
journals.sagepub.com/home/jbf  
 SAGE

Jaykumar Bhasarkar and Dharmendra Bal

## Abstract

Alginate scaffold has been used widely for controlled release applications because of its ability to provide three-dimensional supports for formation of a gel matrix. Alginate gel scaffolds for drug delivery matrices were prepared using a fluidic device. N<sub>2</sub> gas was used in the fluidic device to generate bubbles in the gel layer. The hydrogel matrices with induced voids were compared with hydrogel matrices without voids. This study attempted to identify the release mechanism of vitamin B<sub>12</sub> from the two types of prepared scaffolds, and the data were fitted with different release kinetic models. The results revealed that the alginate scaffold exhibited a controlled release profile and that the corresponding release mechanism followed a first-order kinetic model. Hydrogel scaffolds fabricated with biocompatible polymers using fluidic methods could be promising for controlled drug delivery systems.

## Keywords

Fluidic device, alginate scaffold, vitamin B<sub>12</sub>, drug release kinetics

Date received: 5 July 2018; revised: 10 October 2018; accepted: 9 November 2018

## Introduction

Alginate scaffolds play a major role in the formation of three-dimensional (3D) matrices and have great potential for controlled release applications, making them the subject of extensive research. Use of polymer gel from natural and synthetic sources is now well accepted due to its biocompatibility and the fact that it is biodegradable.<sup>1</sup> The ability of gel layers to hold biological agents and allow their controlled release into a targeted tissue over a long period of time makes them even more promising for further investigation. The gel layer can also act as a scaffold after loading with matrix-forming cells where regeneration of tissue is required.

Recently, many researchers have reported controlled drug delivery using different types of scaffolds. In drug delivery applications, drug uptake is improved by the induction of additional porosity in the alginate gel layer.<sup>2</sup> Moreover, a uniform distribution of this porosity throughout the gel scaffold is essential for optimal function.

Several techniques, such as suspension freeze drying, fiber bonding, gas foaming, thermal phase separation, electro-spinning, and the use of supercritical CO<sub>2</sub>, etc, are used to introduce voids into the gel layer, but these

techniques, in addition to being very expensive, all expose the gel to either thermal or chemical treatment.<sup>3</sup> Direct introduction of bubbles into a thin hydrogel layer by using a fluidic device does not rely on chemical reactions and gives better control to achieve a highly ordered pore structure. Such introduction of bubbles into the gel layer using a micro fluidic device is a simple and good technique to control both void size and the porosity of the scaffold. In this technique, bubbles form and then monodisperse within the scaffold. The self-assembly of bubbles occurs very quickly, forming highly organized structures. The technique is also very economical as compared with other fabrication techniques.

The present study describes the fabrication, using a fluidic arrangement, of an alginate scaffold that can serve as drug delivery device, and the study of its solute release

School of chemical Engineering, Vellore Institute of Technology, Vellore, India

## Corresponding author:

Dharmendra Bal, School of chemical Engineering, Vellore Institute of Technology, SMV Building, Vellore, TN 632014, India.  
Email: dharmendrabal.iitkgp@gmail.com



Creative Commons Non Commercial CC BY-NC: This article is distributed under the terms of the Creative Commons

Attribution-NonCommercial 4.0 License (<http://www.creativecommons.org/licenses/by-nc/4.0/>) which permits non-commercial use, reproduction and distribution of the work without further permission provided the original work is attributed as specified on the SAGE and Open Access pages (<https://us.sagepub.com/en-us/nam/open-access-at-sage>).

behavior and release kinetics. Vitamin B<sub>12</sub> is used as a model drug for kinetic analysis in our study. The proposed method results in an alginic carrier with a uniformly distributed pore structure that influences the uptake and release of drug molecules. With the development of porous hydrogel, sodium alginate has caught the attention of researchers working on drug delivery systems. In recent years, sodium alginate has shown tremendous potential in the pharmaceutical field due to its biodegradability, biocompatibility, and non-toxic properties.<sup>4</sup> Moreover, simple modifications allow fabrication of multifunctional hydrogel structures. Thus, alginate gel is now widely considered for controlled drug delivery release studies.<sup>5-8</sup>

Pluronic F127 is a surfactant that is non-ionic in nature, 100% active, and relatively non-toxic. In general, pluronic F127 is composed of white, waxy, free-flowing granules that are practically odorless and tasteless. It has thermo-responsive properties in aqueous solution. The viscosity of pluronic solution increases with increasing temperature, which has the property of stabilizing the bubbles.

Fabrication of alginate scaffolds using microfluidic techniques has been reported.<sup>9-11</sup> In a fluidic device, two glass capillaries are heated and pulled in such a way that one will be placed inside the other. The gas flow through the inner capillary is pulled by the flowing liquid and breaks to form bubbles. The resulting scaffold, as presented in this paper, is based on the generation of homogeneous bubbles by a co-flow device, where the liquid phase is formed by mixing aqueous polymeric solution with surfactant solution, with N<sub>2</sub> gas being used as the gas phase. The alginate scaffold with embedded voids generated using the above technique forms a non-sticky gel film, where voids distributed homogeneously in the gel scaffold are expected to act as additional reservoirs that can take up a greater amount of drug molecules and hence increase the release rate. Uniformly distributed voids in the gel scaffold can also be useful in the field of tissue regeneration.

The present study reports alginate hydrogel carriers for controlled release of vitamin B<sub>12</sub>. The novelty of this research resides in the following two features: (1) easy and preparation of the gel layer under mild conditions without the use of toxic chemicals; and (2) the introduction of voids using fluidic arrangements that generate highly ordered mono-dispersed bubbles. After optimizing formulation of the alginate gel using the fluidic method, the morphology, mechanical strength, and release kinetics were investigated at different temperatures and with different gel systems.<sup>12-13</sup> Release behavior from hydrogel scaffolds under shaking conditions was also investigated. Furthermore, the release profiles of vitamin B<sub>12</sub> from the different scaffolds were fitted to different kinetic models to reveal release mechanisms.

The main aim of this work was to attempt the fabrication of alginate scaffold using a fluidic device. Vitamin B<sub>12</sub> was selected as the model drug for the study of release

kinetics. The drug release kinetic study investigated the effect on the kinetic rate of surface morphology, varying diameter, drug dissolution, drug loading concentration, etc. The water-soluble model drug inherently followed near first-order kinetics with an initial high release rate. The quantitative and qualitative analysis of the formulation may alter drug release performance. In controlled drug release formulations, analysis of drug dissolution data *in vitro* to anticipate *in vivo* performance is a rational approach.<sup>14</sup> To examine the kinetic release data, we applied the following models:

- (a) Zero-order model
- (b) First-order model
- (c) Higuchi model
- (d) Hixson-Crowell model

## Materials and methods

### Materials

Sodium alginate was purchased from Sigma-Aldrich (St. Louis, MO, USA). The viscosity of 2% solution at 25°C is 250 cP. Pluronic F 127 was purchased from Sigma-Aldrich. The critical micelle concentration of Pluronic F 127 is 4-11. Calcium chloride dihydrate (CaCl<sub>2</sub>·2H<sub>2</sub>O) pellets were purchased from Merck (New Delhi, India). Vitamin B<sub>12</sub> was purchased from SRL (Mumbai, India).

### Methods

An aqueous solution of alginate was prepared by dissolving 4% sodium alginate powder in distilled water. A mechanical stirrer was used at a stirring speed of 2000 rpm for 4 h to dissolve the sodium alginate completely. The pH of the alginate solution was measured and found to be 7.54. An aqueous solution of pluronic F127 surfactant was prepared separately in a beaker by adding 4% of pluronic F127 to distilled water. The mixture was kept on a magnetic stirrer for 1 h at a rotating speed of 300 rpm. The solution was then kept in a refrigerator for 24 h maintained at 4°C for complete dissolution. The pH of the pluronic solution was measured to be 6.56. The resultant solution of alginate and pluronic was prepared by adding alginate and pluronic solution in equal proportions, and mixing in a magnetic stirrer at a rotation speed of 100 rpm for 15 min. The resultant solution maintains a pH of 6.90. The viscosity of the resultant solution was measured at different shear rates at room temperature using parallel plate geometry of a rheometer from Anton Paar.

A co-flow device was fabricated using two glass capillaries pulled by heating. N<sub>2</sub> gas was allowed to flow through the inner capillary and the polymer-surfactant solution was allowed to flow through the outer one. The flow rate of the liquid was controlled by a syringe pump (Figure 1) from Harvard Apparatus (Holliston, MA, USA)

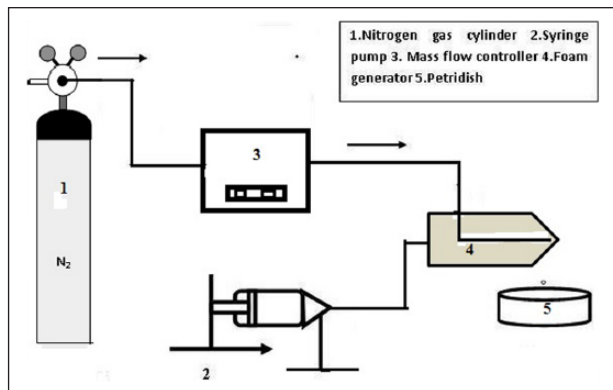


**Figure 1.** Schematic diagram of experimental set up.

and was kept constant throughout the whole experiment. The flow rate of  $N_2$  gas was also maintained constant using a mass flow controller (Alicat Scientific, Tucson, AZ, USA) supplied from a gas cylinder. The flow rates of liquid and gas were maintained at 5.0 ml/min and 1.0 ml/min, respectively. The experimental procedure was described in detail in our previous article.<sup>1</sup> The aqueous film of alginate with entrapped bubbles was collected in a Petri dish for crosslinking with  $CaCl_2$ . Magnified images of the alginate film were captured using a microscope with a camera mounted on it, and the whole system was attached to a computer for continuous monitoring. Davis software from LaVision was used to calculate the diameter of bubbles in the aqueous film. Next, the aqueous solution of  $CaCl_2$  was poured over the alginate film from one side of the Petri dish to form a gel structure within the liquid phase. Excess  $CaCl_2$  solution was removed from the gel structure by dipping it in the distilled water. A scaffold without bubbles was also prepared in a separate Petri dish to allow comparative study of the same composition. The scaffold was then dried in a vacuum oven at a temperature of  $50^\circ C$ ; a constant vacuum pressure of 60 Torr was maintained throughout drying.<sup>15–16</sup> The weight of the scaffold was monitored regularly using a digital weighing balance during the drying period until the weight of the scaffold reached a constant value. A scanning electron microscope (SEM) (JSM 5800; JEOL, Tokyo, Japan) was used to capture images of dried scaffold with and without voids. X-ray diffraction using an x-ray diffractometer (PANalytical, Eindhoven, The Netherlands) was also applied to characterize both types of scaffold (with and without voids). Fe-filtered Co K-alpha 0.178901 nm radiation at 30 mA and 40 kV was used, with a minimum step size of  $2\theta$  as 0.001 and a time per step of 19.685 s.

Next, dried scaffolds with and without voids were dipped separately into a solution consisting of 0.02% vitamin  $B_{12}$  in 0.9% brine solution. At this stage, the objective was to allow the scaffold to absorb the maximum possible amount of vitamin  $B_{12}$  solution. The porosity of the

different types of scaffolds were calculated by gravimetric and volumetric analysis and was presented in our previous article.<sup>1</sup> After uptake, the vitamin  $B_{12}$ -loaded scaffold was taken out slowly from the vitamin  $B_{12}$  solution and immersed in a beaker containing 500 ml of 0.9% brine solution. The beaker was then kept on a vertex shaker with constant shaking at 90 rpm. Samples (5.0 ml) were withdrawn from the beaker at regular intervals during the shaking, and replaced with an equal amount of NaCl solution to maintain a constant volume in the beaker. The absorbance of the collected samples was measured using a UV visible spectrophotometer (Perkin Elmer Lambda 35) at a wavelength of 361 nm. Vitamin  $B_{12}$  concentrations were calculated by comparison with absorbance values of pre-calibrated data from known concentrations.

**Kinetic model for vitamin  $B_{12}$  release studies.** In the present study, a diffusion-based drug delivery system was fabricated and used for loading of vitamin  $B_{12}$  as discussed in our previous articles.<sup>17–18</sup> In all drug release studies, kinetic models make an important contribution to identifying the mechanism of drug release. Many kinetic models have been adopted to discuss the exact mechanism of drug release from different types of supports. We used four different types of kinetic model for vitamin  $B_{12}$  release from different scaffolds. The kinetic models used in this study were: (1) a zero-order kinetic model (2) a first-order kinetic model, (3) the Higuchi model, and (4) the Hixcon-Crowell kinetic model.<sup>19–20</sup>

**Zero-order model.** The zero-order model describes a system where the rate of drug release does not depend on its concentration,

$$Q = Q_0 + k_0 t,$$

where  $Q$  is the amount of drug released from the scaffold,  $Q_0$  is the amount of drug initially present in the solution,  $k_0$  is the rate constant for zero order expressed in concentration/time, and  $t$  is time. Zero-order kinetics defines the process of constant release of drug from the scaffold. Hence, to study drug release kinetics, data was taken from a graph of cumulative drug release vs time. The slope of the above plot gives the zero-order rate constant, and the correlation coefficient data describes whether or not the drug release obeys zero-order kinetics.

**First-order model.** The first-order model describes drug release from the scaffold where the rate of release depends on the concentration of the drug,

$$dC/dt = -k_1 C,$$

where  $k_1$  is the first-order rate constant expressed in  $\text{time}^{-1}$ . This model states that the greater the concentration of the

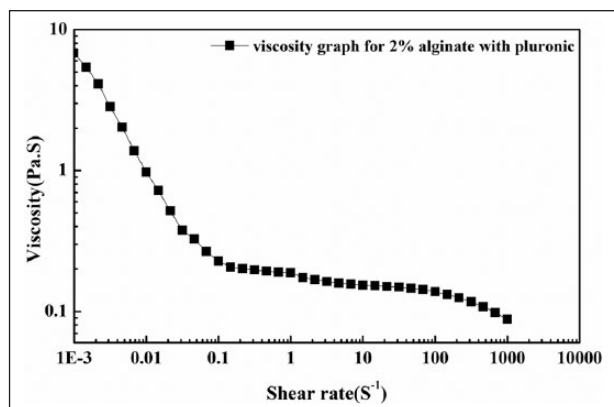


**Figure 2.** Viscosity as a function of shear rate.

drug, the faster the release from the scaffold. The value of the correlation coefficient obtained from the linear plot describes the fitting of first-order kinetics on drug release from the scaffold.

**Higuchi model.** Drug release from a scaffold was described by Higuchi in 1961. The Higuchi model describes the release of drug from the scaffold as the square root of a time-dependent process based on Fick's law of diffusion. It is expressed as

$$Q = kt^{0.5},$$

where  $k$  is a constant.

The data obtained from the drug release from the scaffold is plotted as cumulative percentage of drug release vs the square root of time. The higher value of correlation coefficient describes the diffusion control mechanism of drug release from the scaffold.

**Hixson-Crowell model.** The Hixson-Crowell model describes the release of drugs from a scaffold when there is a change in surface area of the scaffold due to the presence of induced voids.

The relation between drug release and time can be expressed by the equation

$$W_0^{1/3} - W_t^{1/3} = K_{HC}t,$$

where  $W_0$  is the initial amount of drug and  $W_t$  is amount of drug at any time  $t$ .  $K_{HC}$  is the Hixson-Crowell constant.

The kinetic release data obtained from drug release from the scaffold were plotted as the cube root of the percentage of drug remaining in the scaffold vs time.

## Results and discussion

The viscosity data of aqueous alginate solution with pluronic F127 at varying shear rate is depicted in Figure 2.

The results of viscosity measurements show that, with increase in shear rate, the viscosity of the alginate-pluronic solution decreases. This result describes the shear thinning nature of alginate solution after mixing with pluronic F127.

A microscopic image of the alginate bubbles is depicted in Figure 3A. The co-flow device was used to generate bubbles using alginate-pluronic solution as the liquid phase and nitrogen as the gas phase. Image processing using Davis software and computer programs were used to calculate the diameter of the bubbles. The average bubble diameter was found to be 500  $\mu\text{m}$  in the thin film of alginate-pluronic F127. A 4%  $\text{CaCl}_2$  solution was poured into the Petri dish so that the thin film of alginate became a gel.  $\text{Ca}^{+2}$  ions participated in the formation of a 3D network of calcium alginate gel by forming inter-chain ionic bonds. The  $\text{Ca}^{+2}$  ions exchanged rapidly with  $\text{Na}^+$  ions in the alginate to form a gel layer. The aqueous solution of alginate immediately converted into a white milky structure after the  $\text{CaCl}_2$  solution was added, and a free resting non-sticky gel scaffold with embedded voids developed in the Petri dish after a few minutes. The gradual penetration of surplus crosslinking solution into the air bubbles was also observed. A vacuum oven was used to dry the gel film to constant weight to ensure complete drying. Figure 3C presents a SEM image of dry film after complete drying without induced voids, while Figure 3D shows a SEM image of the gel film with induced voids. A reduction in void size was observed after complete drying. The weight and thickness of the film reduced four-fold after drying for all scaffolds, viz, scaffold A, B, C, and D (scaffolds A and C represent scaffolds without bubbles, and scaffolds C and D represent scaffolds with bubbles). Figure 3D clearly shows that the bubbles have been embedded in the alginate scaffold, and that void diameter is reduced from 500  $\mu\text{m}$  to 200  $\mu\text{m}$  due to complete drying. To characterize the alginate scaffold for crystallinity of molecules, XRD was performed (Figure 3B). The broad peak at  $2\theta$  value of  $15.4^\circ$  with  $d$ -spacing of 0.68 nm shows that the composition possesses a low degree of crystallinity or defective crystals. The low crystallinity composition of the molecules leads to proper miscibility and drug dispersion in the alginate scaffold.

After the scaffold had absorbed vitamin  $\text{B}_{12}$ , it was dipped into 0.9% (w/w) brine solution. For analysis of release mechanism of vitamin  $\text{B}_{12}$  from each scaffold, the beaker was kept on a vertex shaker with continuous shaking. Samples were collected at regular intervals for measurement of vitamin  $\text{B}_{12}$  concentration. A volume of brine solution equal to the volume of sample removed was poured into the beaker to make up the solution after every sample collection. A maximum of 1% SD in the calculated drug concentration was expected due to the addition of brine solution to the beaker after collection of each sample. The samples were collected for different scaffolds at regular time intervals to study the release kinetics. The release con-

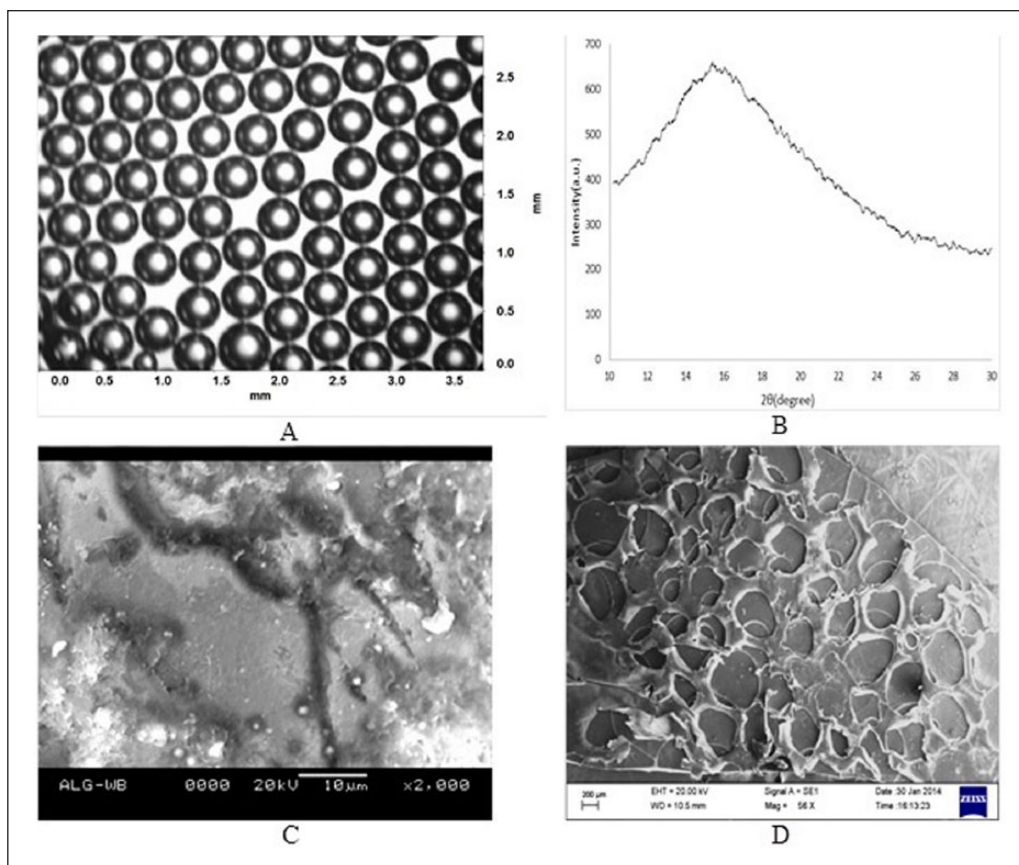


**Figure 3.** (A) Image of aqueous alginate solution under a light microscope. (B) XRD spectrum of alginate scaffold. (C) SEM image of alginate scaffold without bubbles. (D) SEM image of alginate scaffold with bubbles.

centration of vitamin B<sub>12</sub> from different scaffolds was estimated as

$$\begin{aligned} &\text{Release of vitamin B}_{12}\text{ from the scaffold} \\ &= \text{Initial concentration of vitamin B}_{12} \\ &\quad \text{present in the scaffold} \\ &- \text{Concentration of vitamin B}_{12} \\ &\quad \text{remained in the scaffold.} \end{aligned}$$

The amount of vitamin B<sub>12</sub> released from the alginate scaffold was calculated from the amount of vitamin B<sub>12</sub> remaining in the collected sample. The time data plot for the cumulative percentage of vitamin B<sub>12</sub> released from the scaffold is depicted in Figure 4. The amount of vitamin B<sub>12</sub> remaining after 3 h was significantly less for scaffolds with voids. The release rate of vitamin B<sub>12</sub> was enhanced up to four-fold for scaffolds with induced voids compared with scaffolds without induced voids during shaking.

### Vitamin B<sub>12</sub> release mechanism

The time history data of vitamin B<sub>12</sub> released from, and remaining in, the alginate scaffold during the dissolution process was evaluated using a UV-Vis spectrophotometer

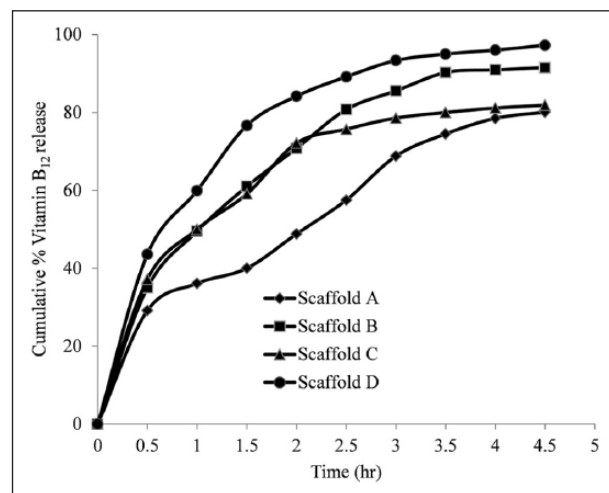


**Figure 4.** Time history data of vitamin B<sub>12</sub> release from different scaffolds.

at  $\lambda_{\max} = 361$  nm; data were fitted to the kinetic models. The value of regression coefficient ( $R^2$ ) was determined by comparing the experimental data with kinetic model data.

From the experimental and model data, the most suitable fit can be suggested by values of  $R^2$  close to 1. In the

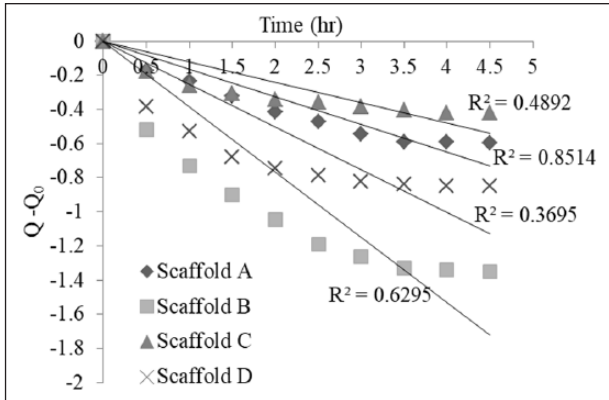


Figure 5. Zero-order kinetic fit for different scaffolds.

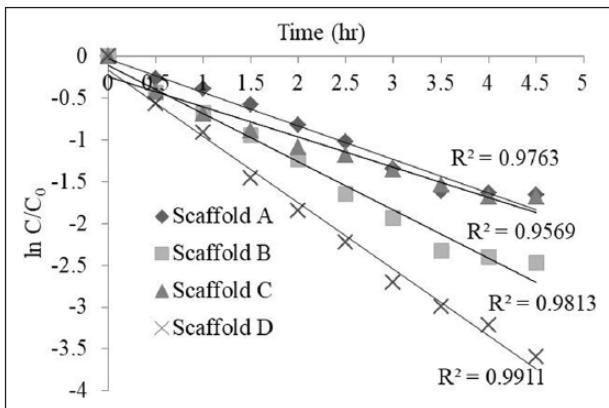


Figure 6. First-order kinetic fit for different scaffolds.

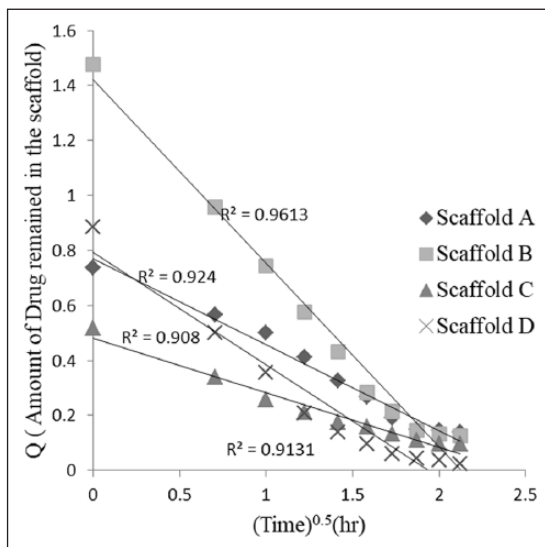


Figure 7. Higuchi kinetic model for different scaffolds.

present study, the zero- and first-order kinetic models were used separately to study the release mechanism of vitamin B<sub>12</sub>, whereas the Hixcon-Crowell kinetic model describes

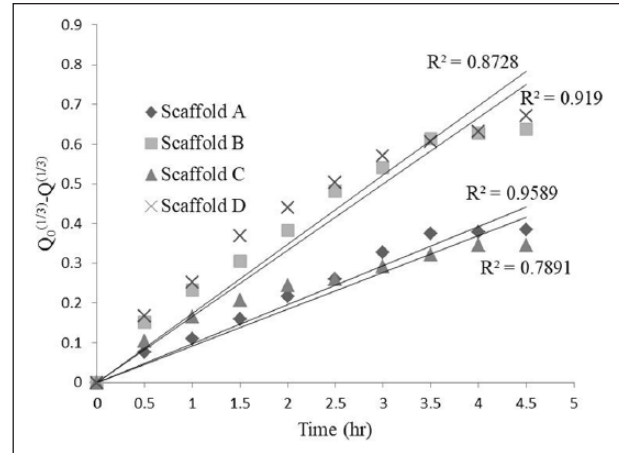


Figure 8. Hixcon Crowell kinetic model for different scaffolds.

drug release due to a dissolution process with variation in diameter and scaffold surface area. The Higuchi model describes the diffusion control mechanism of the alginate scaffold. Kinetic fitted data for zero-order, first-order, the Higuchi, and Hixcon-Crowell models are shown in Figures 5–8, respectively. For the release mechanism of vitamin B<sub>12</sub> from different scaffolds, namely, scaffold A, scaffold B, scaffold C, and scaffold D, higher values of regression coefficient ( $R^2$ ) were obtained from first-order kinetics. The summary of the percentage release of vitamin B<sub>12</sub> and kinetic data for all models with  $R^2$  value are shown in Table 1. The higher value of regression coefficient indicates that the release of vitamin B<sub>12</sub> from all scaffolds followed first-order kinetics. Comparing the reaction rate of vitamin B<sub>12</sub> in scaffold A and scaffold B, scaffold B shows a higher reaction rate than scaffold A. Comparing scaffolds C and D, a higher reaction rate was observed in scaffold D. Overall, the rate constant value ( $k$ ) for scaffold D was ~2-fold higher than scaffold A and ~1.5-fold higher than C. These results indicate that scaffolds B and D show higher release rates than scaffolds A and C, owing to induced voids and higher porosity, as discussed in our previous paper.<sup>2</sup> Higher porosity helps permit greater uptake of vitamin B<sub>12</sub> by the scaffold.

## Conclusions

A drug delivery system based on an alginate hydrogel scaffold was prepared successfully using a CaCl<sub>2</sub> cross-linker. A fabricated micro-fluidic device was used to introduce voids in the gel scaffold. The 500  $\mu$ m void size present in the swollen scaffold reduced to 200  $\mu$ m after drying. The shrinkage in void size affected the absorption and release rate of vitamin B<sub>12</sub>. The scaffold swelled slowly after absorbing vitamin B<sub>12</sub>, and a high cumulative drug release was obtained within 5 h. Different scaffolds showed different release profiles for vitamin B<sub>12</sub>. Scaffold D, which

**Table I.** Kinetic analysis of Vitamin B<sub>12</sub> with different kinetic model.

Scaffold type			Kinetic model			
	% Release	Kinetic parameter	First order	Zero order	Hixcon Crowell model	Higuchi model
Scaffold A	81.0	<i>k</i>	0.4108	0.1626	0.0983	0.31
		<i>R</i> <sup>2</sup>	0.97	0.85	0.96	0.92
Scaffold B	91.5	<i>k</i>	0.611	0.3832	0.167	0.66
		<i>R</i> <sup>2</sup>	0.98	0.63	0.92	0.96
Scaffold C	81.4	<i>k</i>	0.3931	0.1197	0.0926	0.19
		<i>R</i> <sup>2</sup>	0.96	0.50	0.79	0.9
Scaffold D	97.3	<i>k</i>	0.8461	0.2506	0.174	0.40
		<i>R</i> <sup>2</sup>	0.98	0.37	0.88	0.91

contained induced voids, showed a higher percentage release of vitamin B<sub>12</sub> and a higher reaction rate. Scaffolds B and D showed percentage release of >90%, whereas scaffolds A and C showed a percentage release of 80%. Mathematical kinetic models play a major role in interpreting the exact mechanism of drug release from scaffolds. The vitamin B<sub>12</sub> release kinetics in this study were found to be best fitted with first-order kinetics for all scaffolds. The values of most regression coefficients were >0.96 (*R*<sup>2</sup>>0.96), which is good agreement for the best fitting of first-order kinetics for all four types of scaffold. The first-order release kinetics show a significantly slower, and consequently more variable, release rate over time. The first-order kinetics indicate that the release rate of vitamin B<sub>12</sub> depends on its initial concentration. In the case of a scaffold where the initial vitamin B<sub>12</sub> concentration is below its solubility, those vitamin B<sub>12</sub> molecules that diffuse out of the scaffold will decrease with time. Finally, this study shows the utmost importance of using a fabricated scaffold for optimal drug release rate. It can be concluded that alginate scaffolds fabricated by a microfluidic device follow a first-order kinetic profile for controlled drug delivery applications.

### Declaration of conflicting interest

The authors declare no potential conflicts of interest with respect to the research, authorship, and/or publication of this article.

### Funding

The authors received no financial support for the research, authorship, and/or publication of this article.

### References

- Bal D, Patra S and Ganguly S. Use of orifice in throat device to make alginate scaffolds with embedded voids of sub-millimeter tunable dimensions. *Microsyst Technol* 2014; 20: 1359–1364.
- Bal D and Ganguly S. Enhancement of solute release from alginate scaffold with embedded sub-millimeter voids. *J Biomater Sci Polym Ed* 2014; 25: 51–60.
- Chung HJ and Park TG. Surface engineered and drug releasing pre-fabricated scaffolds for tissue engineering. *Adv Drug Deliv Rev* 2007; 59: 249–262.
- Sheridan MH, Shea LD, Peters MC, et al. Bioabsorbable polymer scaffolds for tissue engineering capable of sustained growth factor delivery. *J Control Release* 2000; 64: 91–102.
- Eisult P, Yeh J, Latvala RK, et al. Porous carriers for biomedical applications based on alginate hydrogels. *Biomaterials* 2000; 21: 1921–1927.
- Kolambkar YM, Dupont KM, Boerekel JD, et al. An alginate-based hybrid system for growth factor delivery in the functional repair of large bone defects. *Biomaterials* 2011; 32: 65–74.
- Kuo CK and Ma PX. Ironically crosslinked alginate hydrogels as scaffolds for tissue engineering, part 1. Structure, gelation rate and mechanical properties. *Biomaterials* 2001; 22: 511–521.
- Draget KI, Ostgaard K and Smidsrod O. Homogeneous alginate gels: a technical approach. *Carbohydr Polym* 1991; 14: 159–178.
- Chung K, Mishra NC, Wang C, et al. Fabricating scaffolds by microfluidics. *Biomicrofluidics* 2009; 3: 3122573–3122665.
- Wang X, Li X, Stride E, et al. Novel preparation and characterization of porous alginate films. *Carbohydr Polym* 2010; 79: 989–997.
- Martynov S, Wang X, Stride EP, et al. Preparation of microporous alginate gel using a microfluidic bubbling device. *J Food Eng* 2010; 6: 1556–3758.
- Cong Z, Shi Y, Wang Y, et al. A novel controlled drug delivery system based on alginate hydrogel/chitosan micelle composites. *Int J Biol Macromol* 2018; 107: 855–864.
- Freire M, Fransisco Jr, Marcelino H, et al. Understanding drug release data through thermodynamic analysis. *Materials* 2017; 10: 1–18.
- Dressman JB and Fleisher D. Mixing-tank model for predicting dissolution rate control or oral absorption. *J Pharm Sci* 1986; 75: 109–116.
- Da Silva MA, Bierhalz ACK and Kieckbusch TG. Influence of drying conditions on physical properties of alginate films. *Drying Technol* 2012; 30: 72–79.
- Santagapita PR, Mazzobre MF and Buera MP. Formulation and drying of alginate beads for controlled release and stabilization of invertase. *Biomacromolecules* 2011; 12: 3147–3155.

17. Patra S, Bal D and Ganguly S. Diffusion in and around alginate and chitosan films with embedded sub-millimeter voids. *Mater Sci Eng C Mater Biol Appl* 2016; 59: 61–69.
18. Patra S, Bal D and Ganguly S. Diffusion of moisture from hydrogel scaffold with induced porosity from self-assembled bubbles. *Drying Technol* 2015; 33: 336–345.
19. Bajpai SK and Kirar N. Swelling and drug release behaviour of calcium alginate/poly (sodium acrylate) hydrogel beads. *Des Monomers Polym* 2016; 19: 89–98.
20. Wong BS, Teoh S-H and Kang L. Polycaprolactone scaffold as targeted drug delivery system and cell attachment scaffold for postsurgical care of limb salvage. *Drug Deliv Transl Res* 2012; 2: 272–283.